THE UNIVERSITY OF TEXAS
MD Anderson ~~Cancer~~ Center
Making Cancer History®

Reference and relative dosimetry in magnetic fields

Gabriel O. Sawakuchi
Assistant Professor
Department of Radiation Physics
Division of Radiation Oncology

gsawakuchi@mdanderson.org
www.mdanderson.org/sawakuchilab

Dr. O'Brien, Elekta (former postdoc)

Disclosure

This project was partially funded by Elekta

Learning objectives

1. Understand how the radiation field is affected by the presence of strong magnetic fields
2. Understand how the response of detectors is affected by the presence of strong magnetic fields
3. Understand differences in **relative dosimetry** in the presence of strong magnetic fields
4. Understand differences in **reference dosimetry** in the presence of strong magnetic fields

MR-guided radiation therapy (MRgRT)

- New treatment modality that combines MR-imaging with radiotherapy linacs or Co-60 sources
- Introduces magnetic fields to the radiotherapy environment
- Current range from 0.35 T to 1.5 T
- Magnetic fields change the characteristics of the radiation field and affects the response of detectors

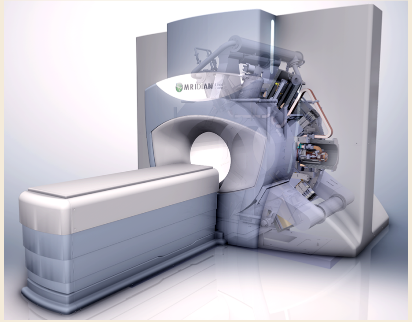

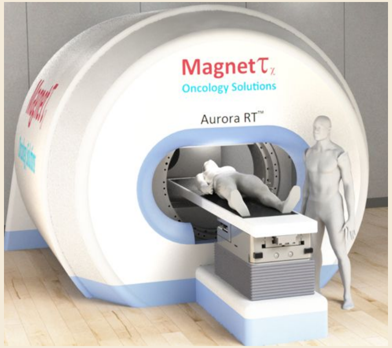

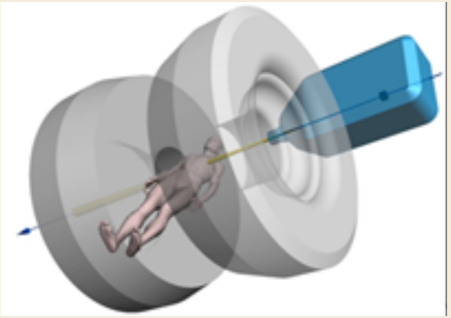

Ingham Institute, Australia

Dosimetry challenges

- Beam data collection is required for the accurate and safe commissioning of the treatment planning system
  - Response of detectors is affected

- Machine calibration using reference dosimetry protocols
  - Geometrical restrictions
  - Adapted protocols

Radiation field is affected by a magnetic field

Lorentz Force

Red: electrons
Blue: positrons

Electrons continue to scatter.

However, their trajectory in water/tissue is heavily influenced by the Lorentz force.

Note: Positrons are deflected in the opposite direction

Radiation field is affected by a magnetic field

Electron Return Effect

Red: electrons
Blue: positrons

No Magnetic Field

1.5 T Magnetic Field

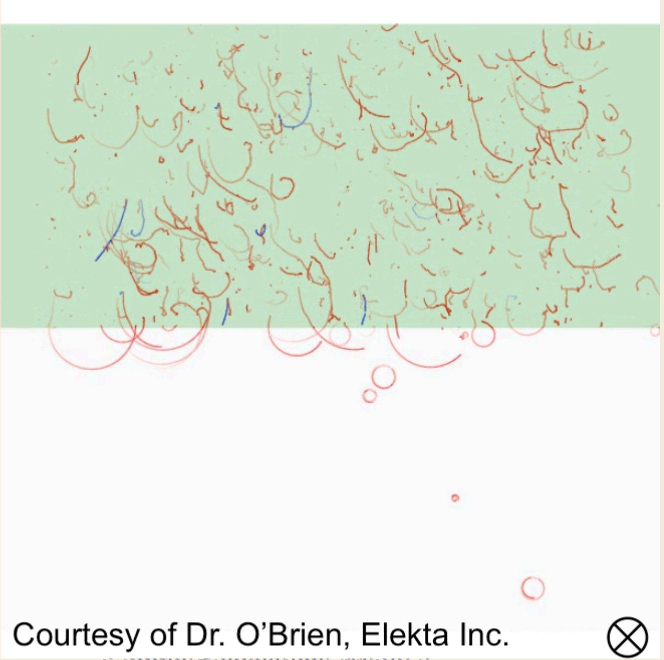

Courtesy of Dr. O’Brien, Elekta Inc.

Electrons return to high density medium

Must to be modelled in the treatment planning system

Radiation field is affected by a magnetic field

Depth dose

- Magnetic field alters the depth dose distribution
- Shifts d_{max} to shallower depths
- Changes the value of the $\%dd(10)_x$ beam quality specifier
- $TPR_{20,10}$ effectively independent of magnetic field strength

Pure Photon Beam	d_{max}	$\%dd(10)_x$	$TPR_{20,10}$
No magnetic field	1.85	71.4	0.697
1.5 T magnetic field	1.30	69.7	0.695

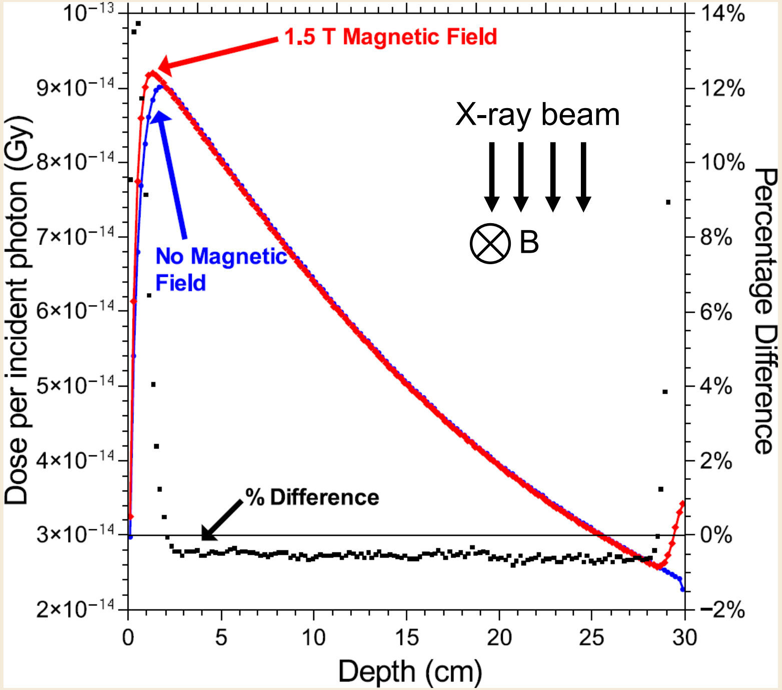

O'Brien et al. (2016). MP 43, 4915

Radiation field is affected by a magnetic field

Lateral profiles

- Magnetic field alters the lateral profiles
- Penumbra becomes asymmetric
- Penumbra becomes broader on one side
- Central axis is shifted

X-ray beam

Scanning direction

⊗ B-field direction

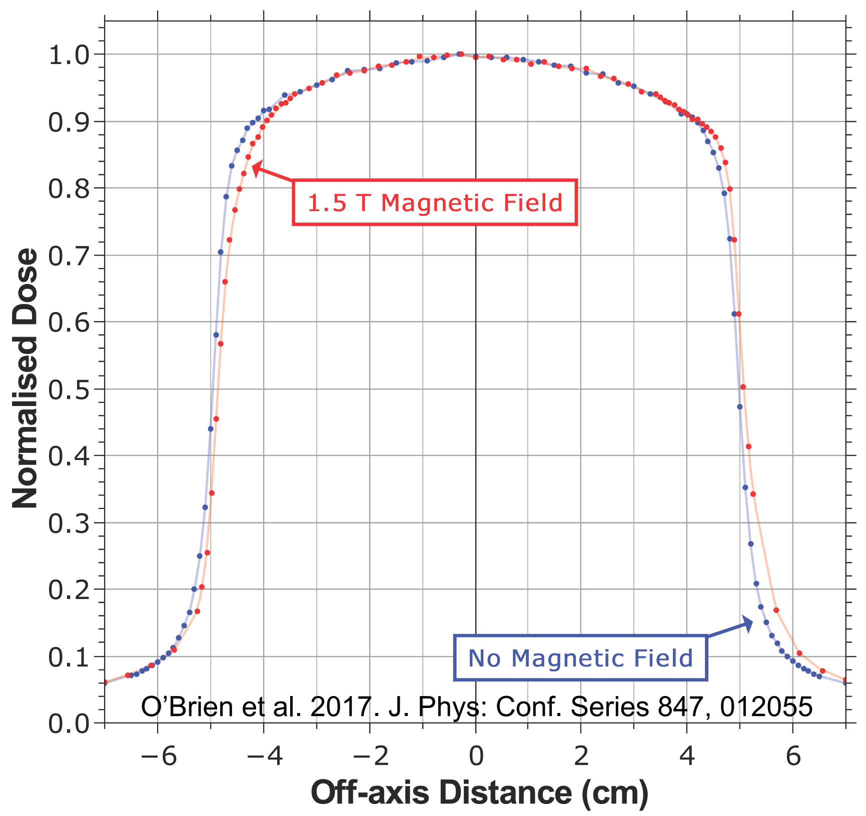

O'Brien et al. 2017. J. Phys: Conf. Series 847, 012055

Detector response is affected by a magnetic field

O'Brien et al. (2017). MP 44, 3830

Air Gap Effect

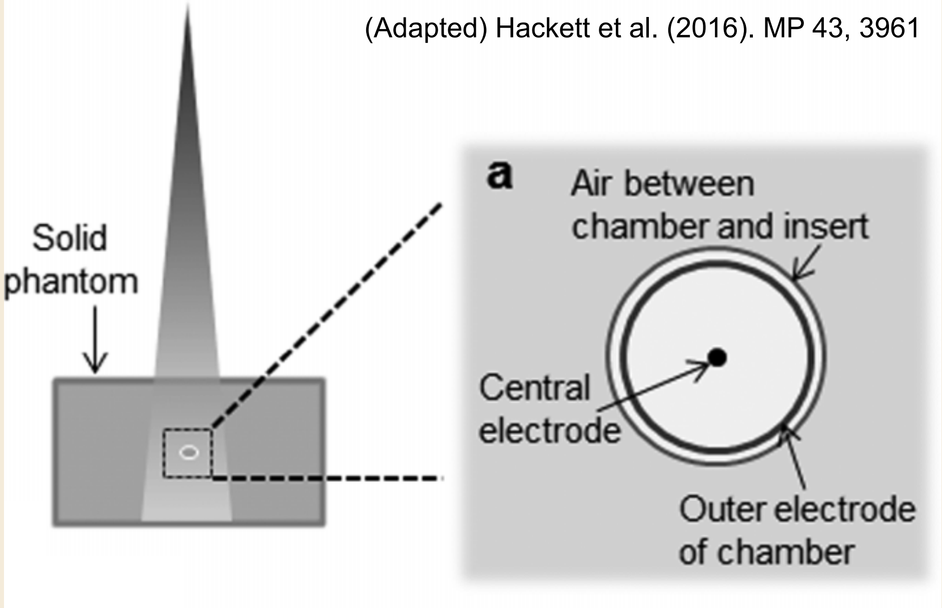

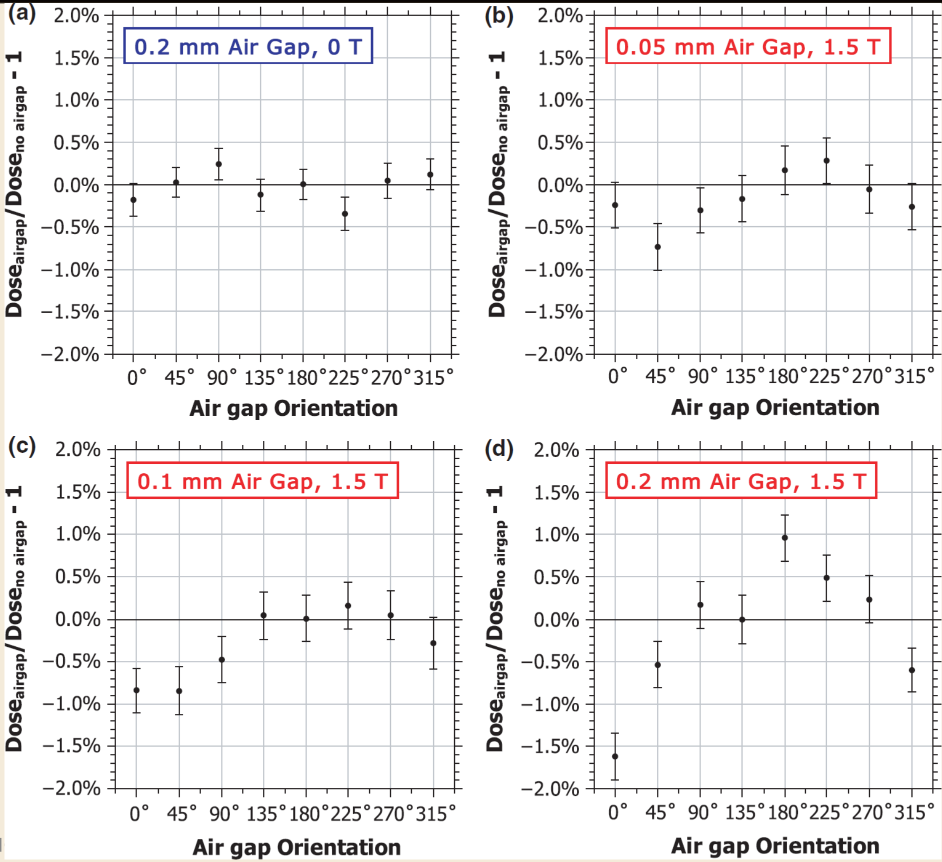

Detector response is affected by a magnetic field

Appropriate detectors to measure dose distributions

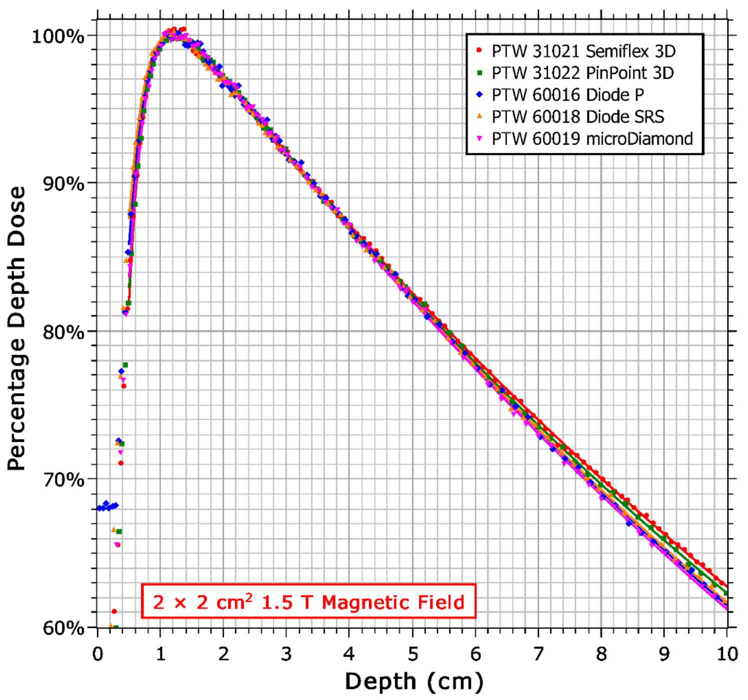

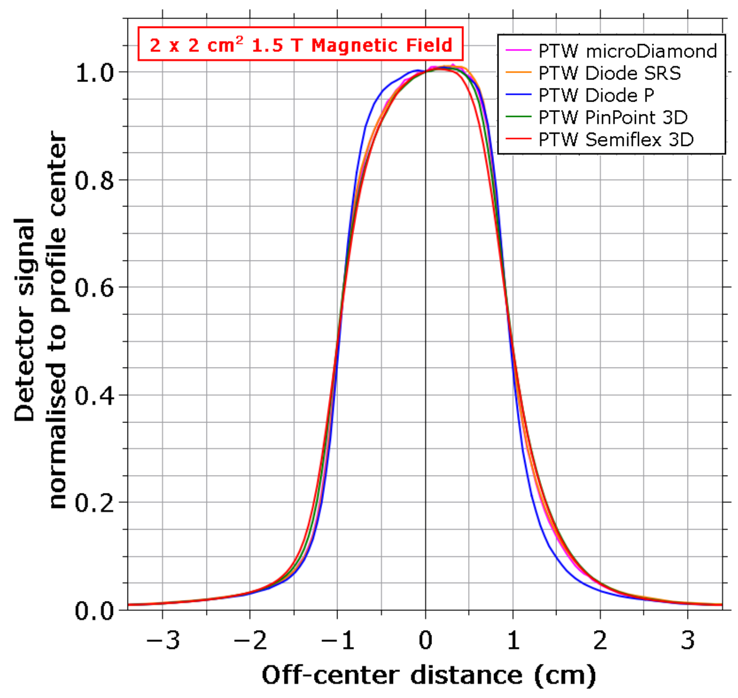

Detector response is affected by a magnetic field

Effective point of measurement (EPOM)

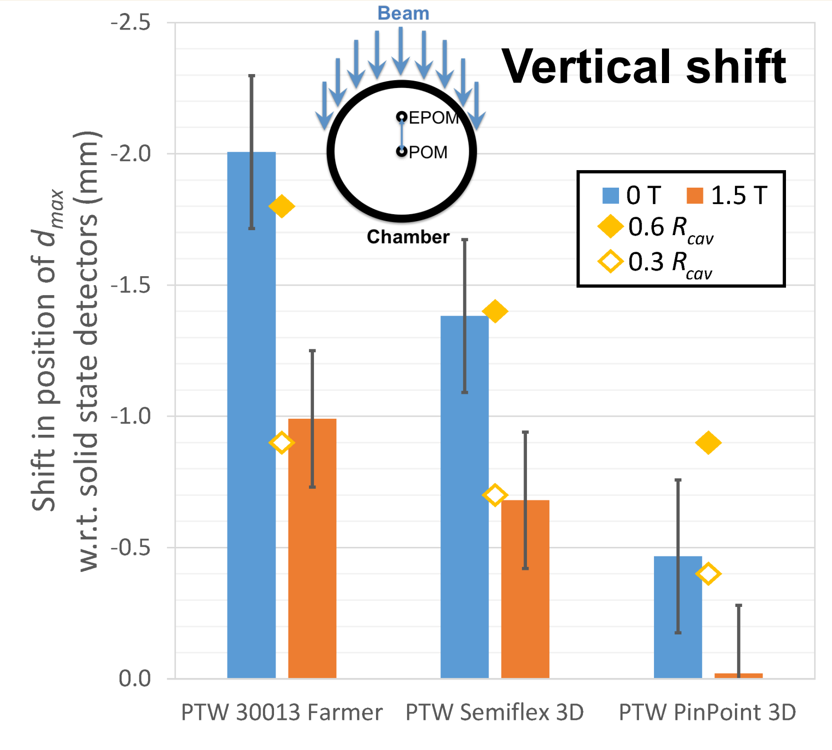

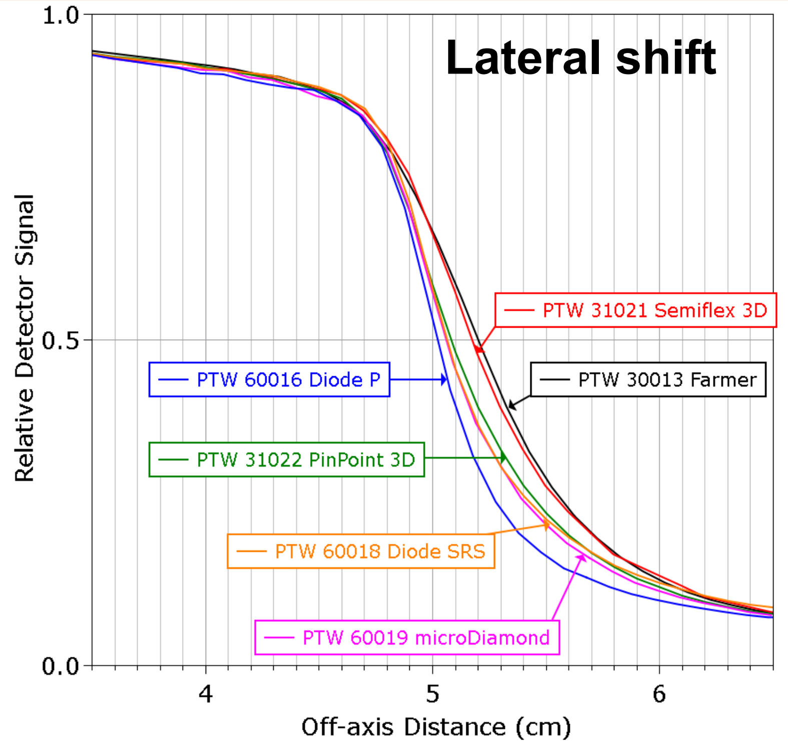

Detector response is affected by a magnetic field

Ionization Chamber Response

Agnew et al. (2017). PMB 62, 1731

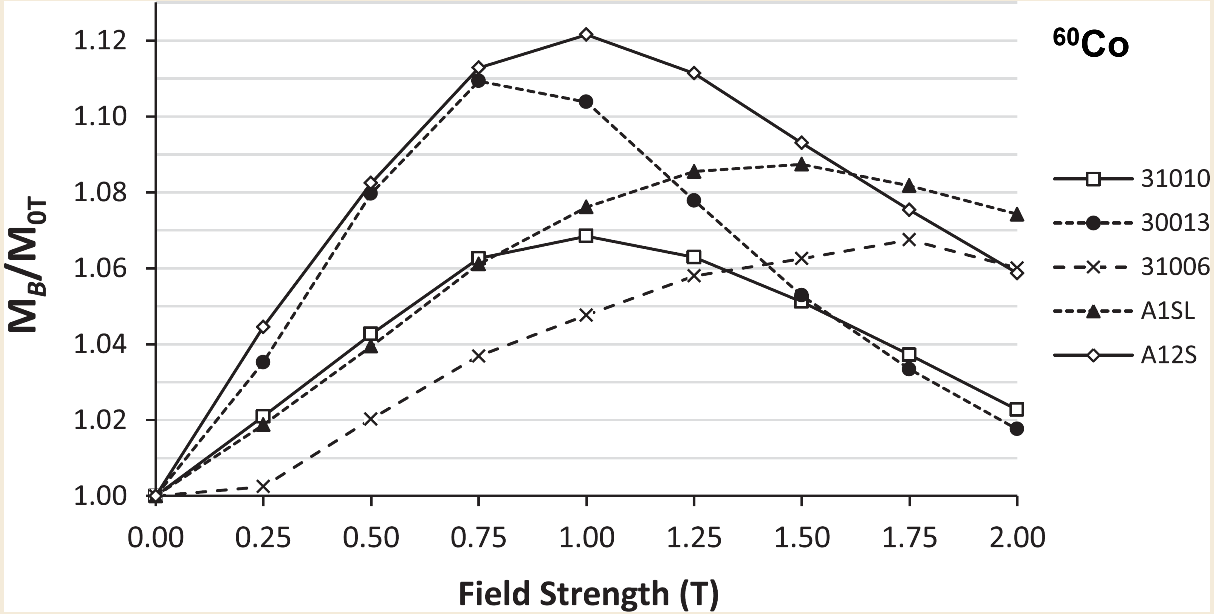

Smit et al. 2013. PMB 58, 5945

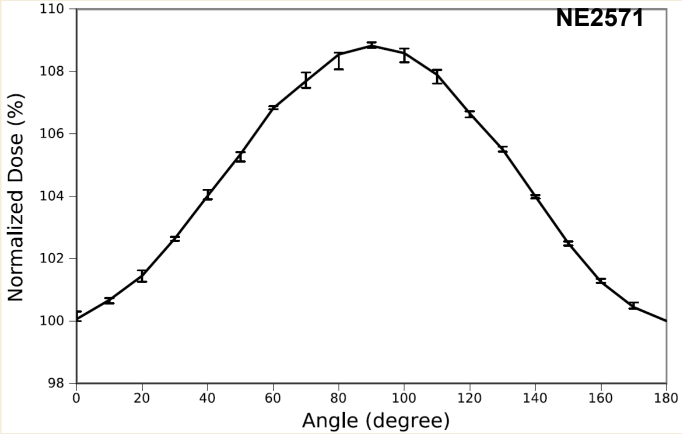

Relative dosimetry

Output factors center versus peak of profile

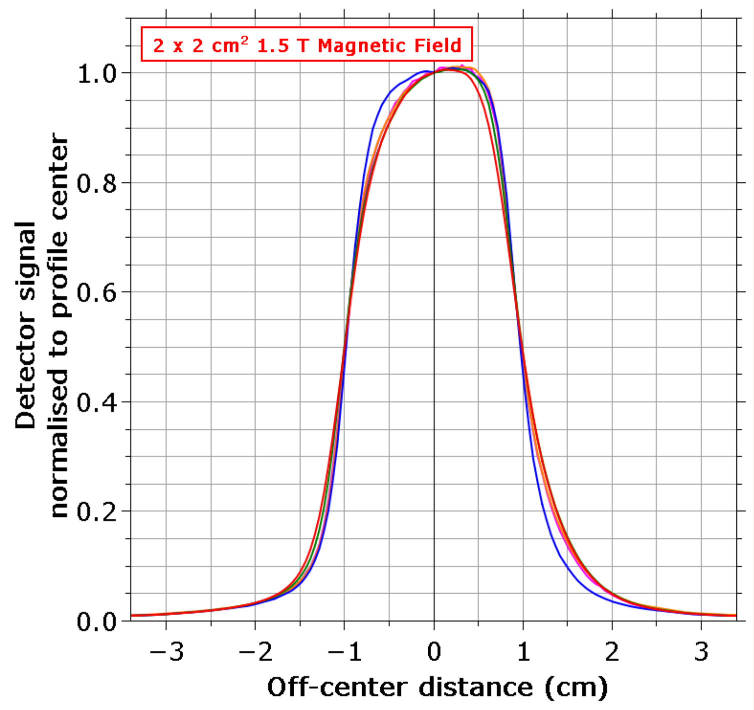

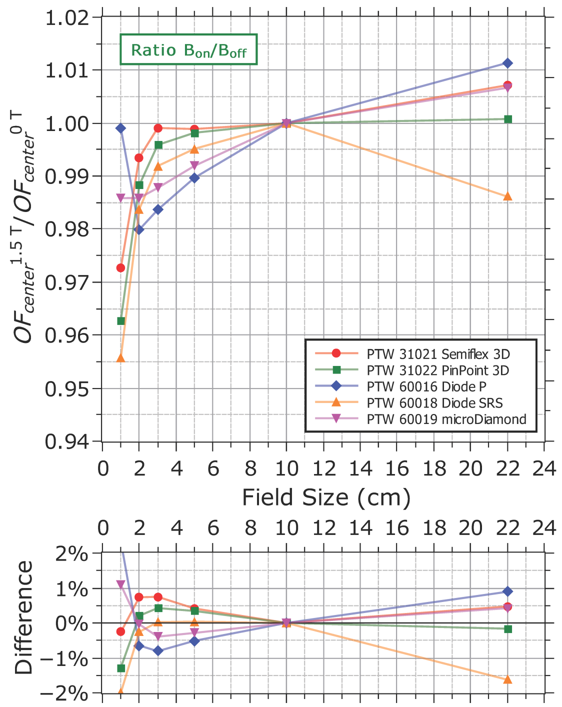

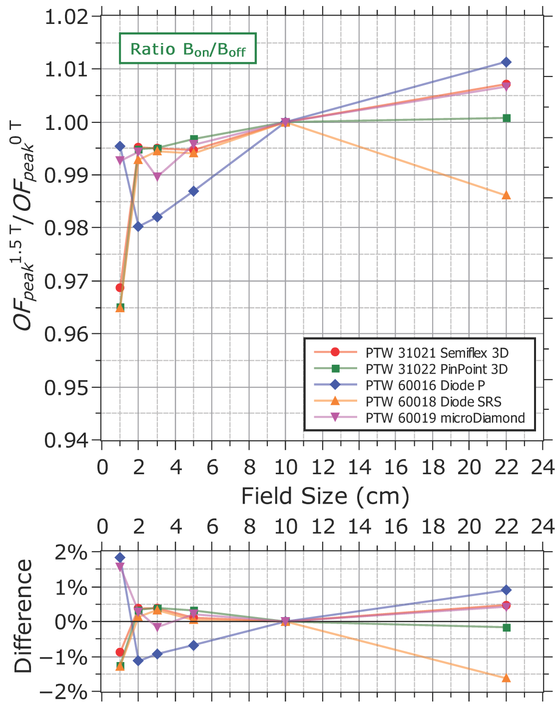

Adaptation strategies

Code of Practices

NPL

Science + Technology | Commercial Services | Educate + Explore | Joint Ventures

Home > News + Events > News

New facility supports development of MRI-guided radiotherapy

A new electromagnet at the National Physical Laboratory's (NPL) Theratron radiation facility will enable research supporting MRI-guided radiotherapy - a state-of-the-art cancer treatment.

Radiotherapy treats cancer by focusing beams of ionising radiation on a tumour, killing cancerous cells by damaging their DNA. Radiation delivery must be tightly controlled to minimise damage to the surrounding healthy tissue. Typically, X-ray based techniques are used to image a patient immediately before treatment to direct the radiation. But tumours move and deform inside a patient's body with bodily functions such as breathing, and can shift and change in size over the course of treatment.

MRI-guided radiotherapy provides real-time images during a patient's treatment, and offers more detailed and higher contrast images for the identification of tumours and soft tissues. This boosts tumour targeting accuracy, reducing side-effects and increasing survival rates. Currently untreatable cancers, such as kidney and pancreatic tumours, which can't be accurately tracked during treatment, may become treatable.

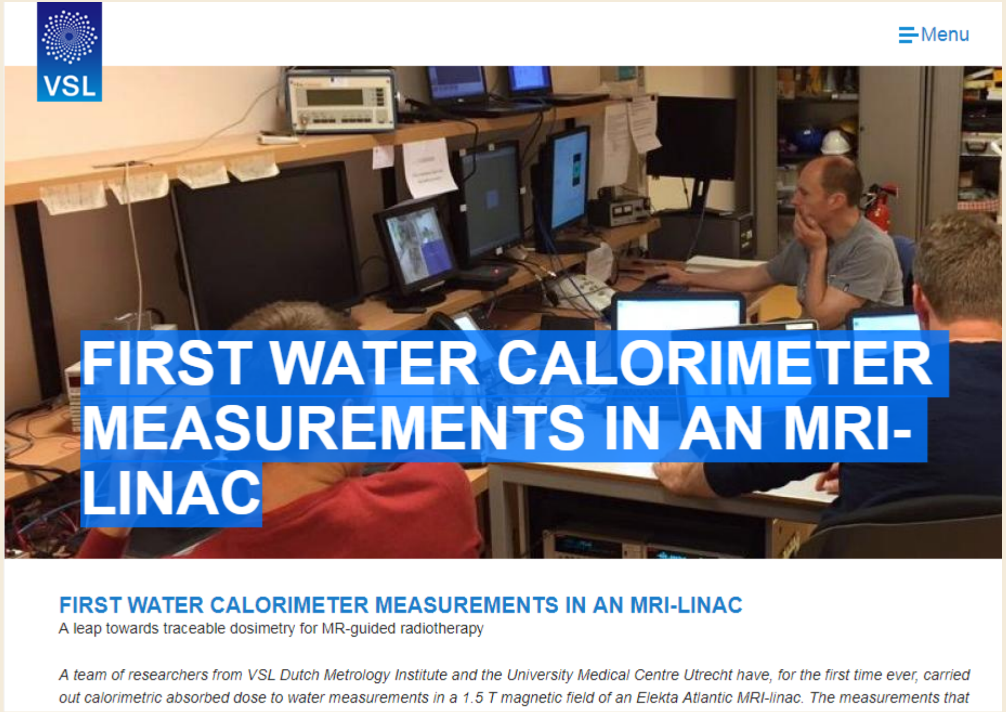

VSL

Menu

FIRST WATER CALORIMETER MEASUREMENTS IN AN MRI-LINAC

FIRST WATER CALORIMETER MEASUREMENTS IN AN MRI-LINAC

A leap towards traceable dosimetry for MR-guided radiotherapy

A team of researchers from VSL Dutch Metrology Institute and the University Medical Centre Utrecht have, for the first time ever, carried out calorimetric absorbed dose to water measurements in a 1.5 T magnetic field of an Elekta Atlantic MRI-linac. The measurements that

Adaptation strategies

Dose to Water

- **NPL using Alanine**
- **Calorimetry**
  - **Water calorimetry (VSL)**
  - **Miniature graphite calorimetry (Sunnybrook)**

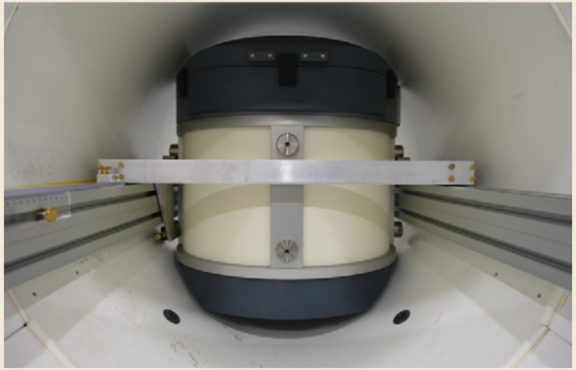

L de Prez et al. (2016). PMB 61, 5051

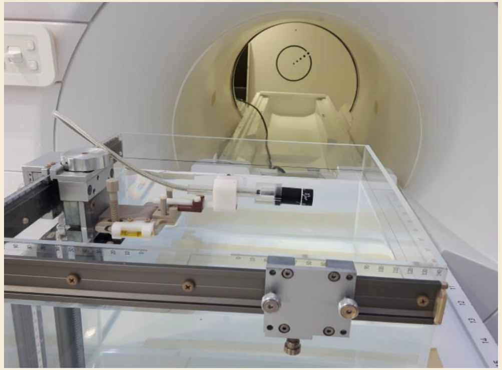

Courtesy of Dr. Sarfehnia

Adaptation strategies: reference dosimetry

Formalisms

Current dosimetry formalisms do not account for the effect of the magnet field on the ionization chamber response:

Original Formalism	$D_w^Q = M \cdot N_{D,w}^{^{60}Co} \cdot k_Q$	AAPM, IAEA, …
Adapted Formalisms	$D_w^Q = M \cdot N_{D,w}^{^{60}Co} \cdot k_Q \cdot k_B^Q$	(O'Brien et al. 2016) (Malkov & Rogers 2018) (Spindeldreier et al. 2017)
	$D_w^Q = M \cdot N_{D,w}^{^{60}Co} \cdot k_Q \cdot c_B \cdot {}'k_B^Q$	(van Asselen et al. 2018)

k_B^Q (or k_B) is difficult to measure. Monte Carlo difficult to validate empirically.

Adaptation strategies: reference dosimetry

Ionization Chamber Orientation

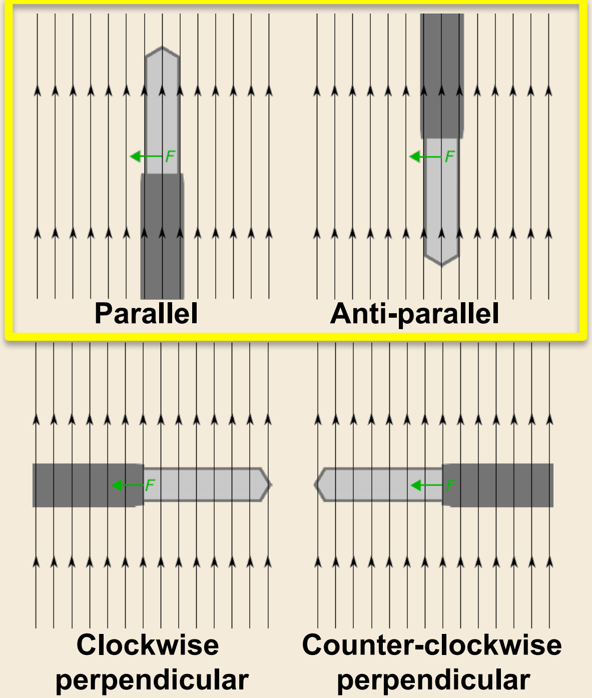

O'Brien et al. (2016). MP 43, 4915

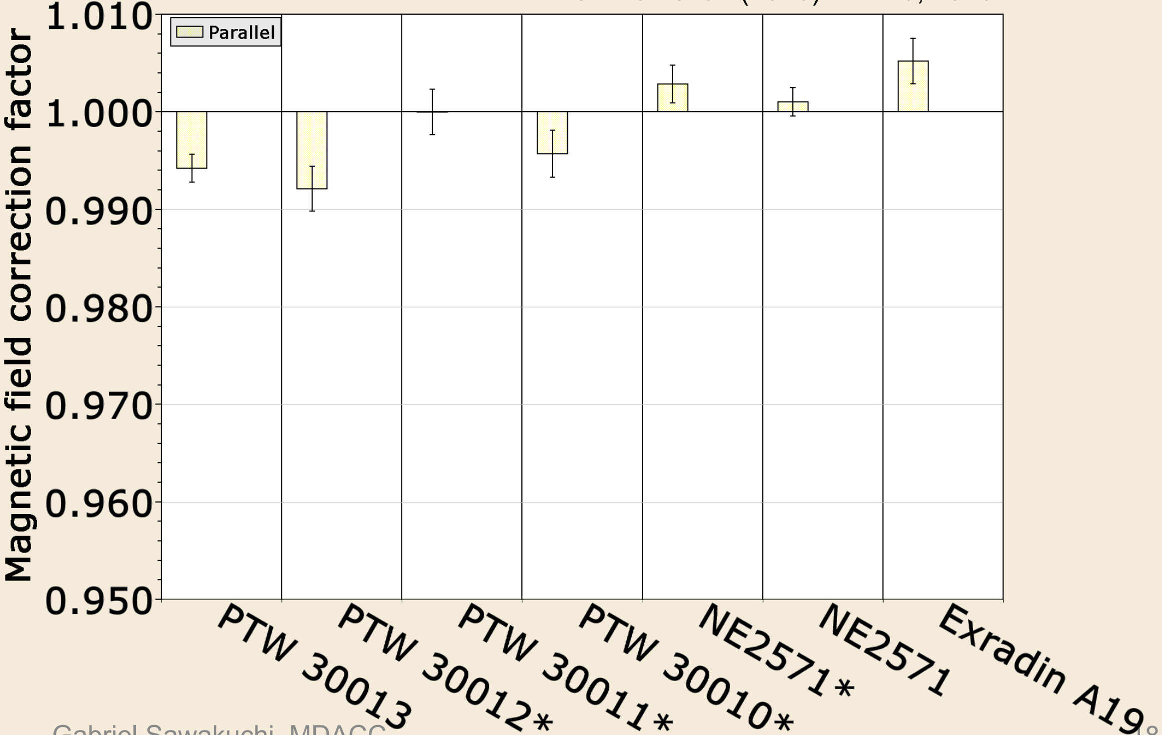

Adaptation strategies: reference dosimetry

Ionization Chamber Orientation

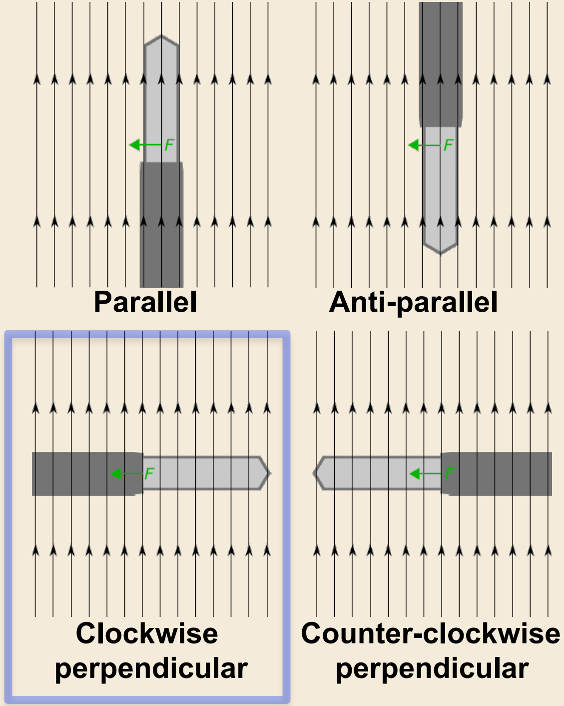

O'Brien et al. (2016). MP 43, 4915

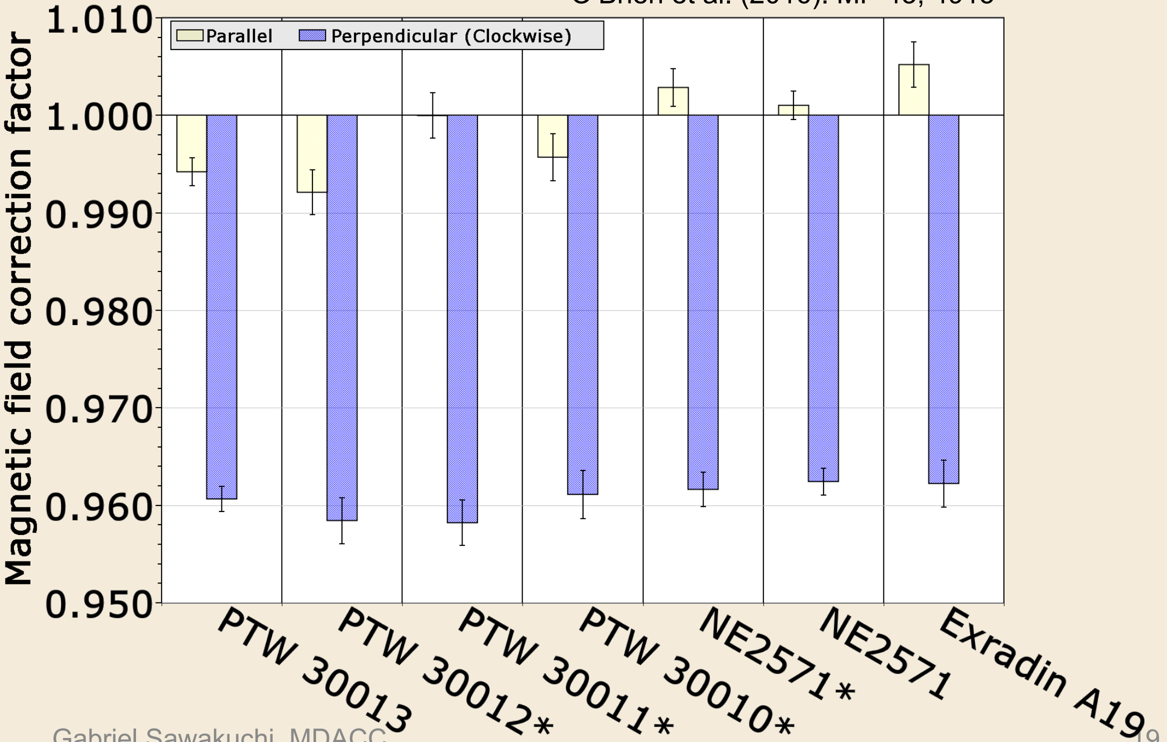

Adaptation strategies: reference dosimetry

Ionization Chamber Orientation

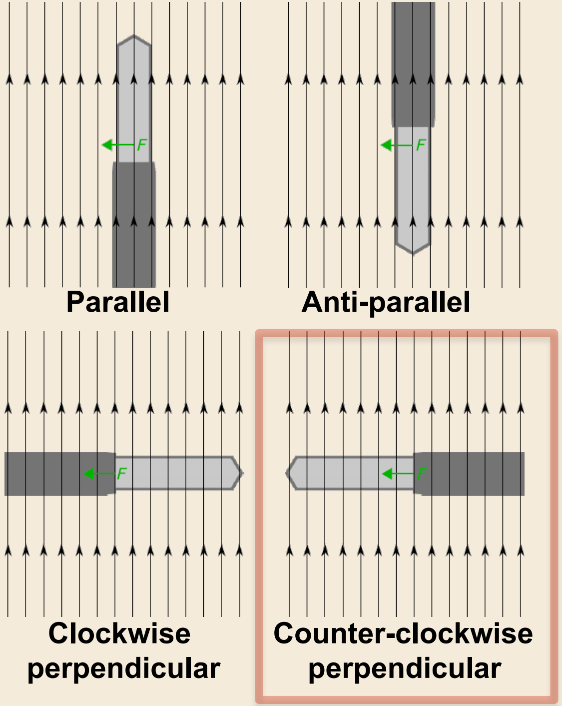

O'Brien et al. (2016). MP 43, 4915

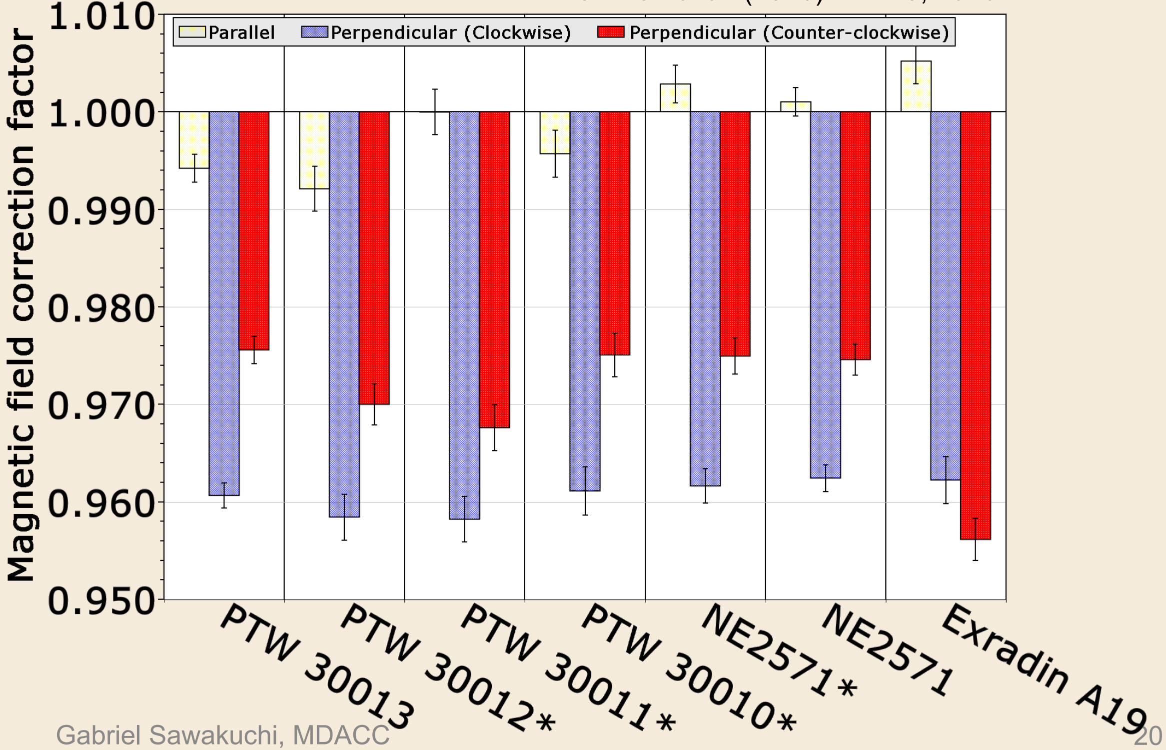

Adaptation strategies: reference dosimetry

k_B versus Beam Quality

$||_{ch}$: magnetic field parallel to chamber
$||_{ph}$: magnetic field parallel to photon beam

***$TPR_{20,10}$* is independent of the magnetic field**

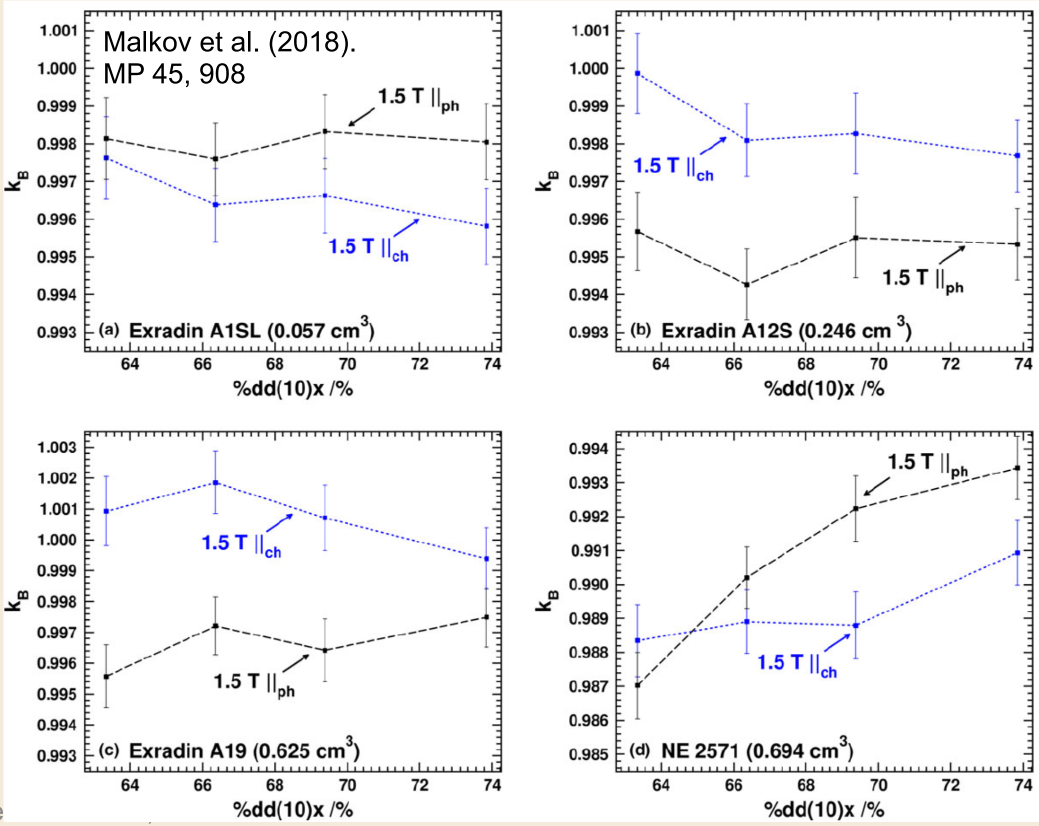

Adaptation strategies: reference dos

Published Values of k_B

NE2571 Characteristic	Without magnetic field: Average value	Without magnetic field: Maximum deviation	With magnetic field: Average value	With magnetic field: Maximum deviation
Linearity	100.1%	0.4%	100.1%	0.2%
Repeatability	0.1%	<0.1%	0.1%	<0.1%
P_{ion}			1.001	<0.001
P_{pol}	1.000	<0.001	1.000	<0.001
$P_{1.5\,T}$ (perpendicular)			0.953	0.002

Smit et al. 2013. PMB 58, 5945

O'Brien et al. 2016. MP 43, 4915

Detector	$k_{B_\parallel}^{Q_{msr}}$	$k_{B_\curvearrowleft}^{Q_{msr}}$	$k_{B_\curvearrowright}^{Q_{msr}}$	Uncertainty (%)
PTW 30013	0.994	0.961	0.976	0.15
PTW 30012[a]	0.992	0.958	0.970	0.25
PTW 30011[a]	1.000	0.958	0.968	0.25
PTW 30010[a]	0.996	0.961	0.975	0.25
NE2571[a]	1.003	0.962	0.973	0.20
NE2571	1.001	0.962	0.973	0.15
Exradin A19	1.005	0.962	0.956	0.25

[a]Chambers modeled with a 1 mm thick layer of PMMA representing a water-proof sleeve.

Chamber type	Reference		$TPR_{20,10}$	$k_{B_\perp,Q}$	$k_{B_\parallel,Q}$
PTW 30013	UMC Utrecht	M	0.701	0.963(2)	0.992(2)
	de Prez *et al* (2016b)	M	0.702	0.961(7)	
	O'Brien *et al* (2016)	MC	0.695	0.976(1)	0.994(1)
				0.961(1)[a]	
	Malkov *et al* (2017a)	MC	0.695		0.988(1)
	Spindeldreier *et al* (2017)	MC	0.674	0.954(3)	0.993(3)
				0.959(3)[a]	
IBA FC65-G	UMC Utrecht	M	0.701	0.952(2)	0.997(3)
	de Prez *et al* (2016b)	M	0.702	0.951(7)	
	Malkov *et al* (2017a)	MC	0.695		0.992(1)

[a] Result obtained with chamber in the perpendicular orientation as shown in figure 2, but with the magnetic field in the opposite direction.

van Asselen et al. 2018. PMB 63, 125008

Reynolds et al. 2017 MP 44, 4322

$'k_B^Q$ (1.5 T): PR06C	
Perpendicular	Parallel
0.953 ± 0.008	0.996 ± 0.008

Malkov & Rogers 2018. MP 45, 908

chamber $[V(cm^3)]$	k_B (1.5 T) $\parallel_{ch}$	$\parallel_{ph}$
A12 (0.65)	0.9983	0.9940
A19 (0.62)	1.0007	0.9964
A2 (0.54)	0.9989	0.9952
T2 (0.54)	1.0004	0.9999
A12S (0.25)	0.9984	0.9962
A18 (0.125)	0.9981	0.9971
A1(0.057)	0.9962	0.9983
A1SL (0.057)	0.9966	0.9983
A14* (0.016)	**0.9718**	**0.9827**
T14*(0.016)	**0.9696**	**0.9837**
A14SL* (0.016)	**0.9725**	**0.9823**
A16* (0.016)	**0.9600**	**0.9830**
30010^w (0.6)	**0.9872**	0.9932
30011^w (0.6)	0.9920	1.0009
30012^w (0.6)	**0.9870**	0.9938
30013 (0.6)	**0.9881**	0.9937
31006 (0.015)	**0.9867**	0.9953
31010 (0.125)	0.9933	0.9905
31016 (0.016)	0.9963	0.9992
31014 (0.015)	0.9951	0.9992
FC65-G (0.65)	0.9917	0.9914
FC65-P (0.65)	0.9917	0.9901
FC23-C (0.23)	0.9980	0.9972
CC25 (0.25)	0.9987	0.9968
CC13 (0.13)	0.9990	0.9969
CC08 (0.08)	0.9975	0.9973
CC04 (0.04)	0.9971	0.9998
CC01 (0.01)	**0.9805**	**0.9889**
NE2581^w (0.6)	0.9993	1.0011
NE2571^w (0.6)	**0.9888**	0.9922
NE2561^w (0.325)	0.9963	**0.9875**
PR06C/G^w (0.65)	0.9986	0.9973

Final remarks

- Radiation field is affected by the presence of a strong magnetic field
    - Depth dose distribution
    - Lateral profile
    - Ionization density
- Detector response is affected by the presence of a strong magnetic field
    - Air gap
    - Shielding effects
    - Detector orientation
- New strategies must be adopted to perform relative dosimetry
- Adapted formalisms and new detectors are required to calibrated MRgRT units that employ strong magnetic fields

Thank you! Questions?

gsawakuchi@mdanderson.org

Sawakuchi Lab
Sharmistha Chakraborty, Research Scientist
Scott Bright, Postdoc
Racheal Martin, Physics Resident
Conor McFadden, Sr Research Engineer
David Flint, PhD student
David Yoon, RAII
Hatim Amiji, Undergrad student, Rice University
Zac Metzler, AAPM summer student
Sruthi Sivabhaskar, MD Anderson summer student

Daniel J. O’Brien, Postdoc, former member

MD Anderson
David Grosshans
Radhe Mohan
Narayan Sahoo
Cullen Taniguchi
Pablo Yepes
Uwe Titt
Dragan Mirkovic

External Collaborators
Asaithamby Aroumougame, UTSW
Steffen Greilich, DKFZ
Teruaki Konishi, NIRS
Satoshi Kodaira, NIRS
Yoshiya Furusawa, NIRS
Mark Akselrod, Landauer Inc
Joseph Duman, BCM
Pavel Sumazin, BCM

Funding
Elekta, CPRIT, UTSW and NCI